Available online at www.sciencedirect.com
SCIENCE DIRECT
ELSEVIER
Journal of the European Ceramic Society 26 (2006) 647–653
ECERS
www.elsevier.com/locate/jeurceramsoc

# Preparation of single crystalline $Sr_{0.5}Ba_{0.5}Nb_2O_6$ particles

Weiwu Chen [a,*], Shoichi Kume [a], Cihangir Duran [a,b], Koji Watari [a]

[a] *Advanced Manufacturing Research Institute, National Institute of Advanced Industrial Science and Technology (AIST), Anagahora 2266-98, Shimoshidami, Moriyama-ku, Nagoya 463-8560, Japan*
[b] *Gebze Institute of Technology, Materials Science and Engineering Department, P.K. 141, 41400 Gebze-Kocaeli, Turkey*

Available online 1 August 2005

**Abstract**

Single crystalline and agglomerate-free ceramic particles are important for fabrication of grain-oriented ceramics by the self-assemble processes. In the present work, preparation of single crystalline $Sr_{0.5}Ba_{0.5}Nb_2O_6$ particles was first explored by traditional solid-state reaction and molten-salt synthesis methods. The results show that the particles synthesized by solid-state reaction were spherical, hard-aggregated and polycrystalline. Molten salt synthesis provides sub-micrometer anisotropic single crystalline $Sr_{0.5}Ba_{0.5}Nb_2O_6$ particles and the morphology of a particle may be adjusted by changing synthesis conditions. The synthesized particles have uniform size distribution and are easily dispersed, thus may suit self-assemble processes to prepare grain-oriented ceramics. Furthermore, effects of synthesis conditions in molten salt synthesis, on the phase formation, morphology and size distribution of SBN particles were investigated.


*Keyword:* $Sr_{0.5}Ba_{0.5}Nb_2O_6$; Electron microscopy; Functional applications

## 1. Introduction

Functional ceramics and single crystals are being used in many applications in electronics and optics due to their one or more special physical properties in dielectric, piezoelectric, pyroelectric, ferroelectric and electro-optic behaviors. Compared to single crystals, ceramics are easily fabricated and very inexpensive, but their physical properties are much poorer than that of the corresponding single crystals. This is because the random grain orientation in ceramics leads to poor poling quality and inhibits the appropriate orientation of the polarization axes. Therefore, it is desirable to obtain ceramics with oriented grains according to their physical properties. Recently, some self-assemble processes in ceramics, such as templated grain growth (TGG)[1–3] and magnetic alignment (MA)[4,5] techniques were developed for this purpose. In these processes, part or all starting particles are aligned according to their anisotropic properties and then form dense grain-oriented ceramics with properties close to the single crystals after sintering. In TGG processing, large anisotropically-shaped template particles were oriented by external mechanical force in a fine-grained matrix in green body, and then a textured microstructure is developed by growth of aligned particles during sintering and post heat treatment. In MA processing, the single crystalline particles with feeble magnetic susceptibility may be aligned in a high magnetic field through the colloidal processing. So, anisotropic single crystalline particles play a decisive role on the properties of final sintered ceramics in these processes. The requirement for particles may be different in various processes, but generally they should be single crystalline, homogenous size distribution, easily dispersed and anisotropic shape or physical properties.

$Sr_xBa_{1-x}Nb_2O_6$ (SBN, where $x = 0.25$–$0.75$) ferroelectric materials with tungsten bronze structure have excellent pyroelectric, linear electric-optic coefficients, photo refractive effects and interesting piezoelectric properties.[6,7] The tungsten bronze structure consists of a skeletal framework of $MO_6$ octahedra, sharing corners to form three types of tunnels parallel to the *c*-axis in the unit cell formula of $[(A_1)_2(A_2)_4C_4][(B_1)_2(B_2)_8]O_3$, in which the 12-coodinated $A_1$ site, 15-coordinated $A_2$ site, 9-coodinated C sites, and 6-coodinated $B_1$ or $B_2$ sites, may be occupied by corresponding

* Corresponding author. Tel.: +81 52 736 7158; fax: +81 52 736 7405.
*E-mail address:* weiwu.chen@aist.go.jp (W. Chen).

0955-2219/$ – see front matter © 2005 Elsevier Ltd. All rights reserved.
doi:10.1016/j.jeurceramsoc.2005.06.010

cations, respectively. In SBN, The $Ba^{2+}$ ion (1.74 Å) predominantly occupies the bigger 15-coordinated $A_2$ sites, and the $Sr^{2+}$ ion (1.54 Å) occupies the $A_1$ or a combination of $A_1$ and $A_2$ sites depending on the compositions. The $B_1$ and $B_2$ sites are occupied by $Nb^{5+}$ ions.[8] Because SBN crystals have obvious anisotropic properties, the attempts to prepare grain-oriented SBN ceramics were tried in recent years. Nagata et al.[9] achieved anisotropic SBN ceramics by hot pressing, but the polarization values were very below the single crystal values. Duran et al.[2] prepared high grain-oriented SBN ceramics via TGG, however the acicular $KSr_2Nb_5O_{15}$ (KSN) particles were used as templates, which introduced more $K^+$ ions into the SBN lattice.

Several wet chemical techniques have been investigated to synthesize SBN powders,[10–12] but most attentions were focused on the effect of synthesis temperature and particle size. In addition, expensive organic salts were required in these techniques. Molten salt synthesis (MSS) is a well-established, low-cost technique of forming a desirable compound in a flux of low melting point.[13] The size and morphology of resulting particles are easily controlled by synthesis conditions. Some ceramic powders, such as $Sr_2Nb_2O_7$,[14] $BaFe_{12}O_{19}$,[15] $BaNd_2Ti_4O_{12}$[16] and lead-based niobates[17–19] have been obtained by MSS technique. But few open literatures reported the molten salt synthesized SBN.

In the present work, preparation of single crystalline $Sr_{0.5}Ba_{0.5}Nb_2O_6$ particles, suitable for self-assemble processes, was explored by molten salt synthesis method. For comparison, solid-state reaction method was also used. Effects of synthesis conditions, such as salt amount, temperature, soaking time and cooling rate, on the morphology and size distribution were investigated in detail. TEM and EDS were also employed to characterize the single crystalline SBN particles.

## 2. Experimental

### 2.1. Preparation of SBN particles

The nominal composition of SBN was $Sr_{0.5}Ba_{0.5}Nb_2O_6$ (SBN50). The starting materials used were $BaCO_3$ (99%), $SrCO_3$ (99%), $Nb_2O_5$ (99%), NaCl (99.5%) and KCl (99.5%). According to the reaction (1), the stoichiometric amount of $BaCO_3$, $SrCO_3$ and $Nb_2O_5$ were mixed by planetary mill for 1 h in ethanol medium, and then dried at 110 °C for 2 h. In solid-state reaction method, the mixed powders were synthesized in air directly at designed temperature for 4 h at a heating rate of 4 °C/min. In molten-salt synthesis, the salt was equal molar ratio NaCl–KCl, and two compositions were designed: SBN-1 (SBN and salt with 1:1 weight ratio) and SBN-2 (SBN and salt with 1:2 weight ratio). The mixture of starting powders of SBN50 were mixed with salt by hand-ground in a mortar and pestle for 30 min and then heated to designed temperature at a rate of 4 °C/min. The detail sample compositions and synthesis conditions are listed in Table 1. As-synthesized SBN particles by MSS were washed several times with deionized water until no free chloride ions were detected by silver nitrate solution.

Table 1
SBN50 samples synthesized by MSS

| Samples | Weight ratio of SBN and salt | Synthesis conditions (temperature, duration and cooling rate) |
|---|---|---|
| SBN-1-1 | 1:1 | 950 °C, 4 h and 2 °C/min |
| SBN-1-2 | 1:1 | 1000 °C, 4 h and 2 °C/min |
| SBN-1-3 | 1:1 | 1000 °C, 4 h and 10 °C/min |
| SBN-1-4 | 1:1 | 1000 °C, 10 min and 10 °C/min |
| SBN-2-1 | 1:2 | 950 °C, 4 h and 2 °C/min |
| SBN-2-2 | 1:2 | 1000 °C, 4 h and 2 °C/min |
| SBN-2-3 | 1:2 | 1000 °C, 4 h and 10 °C/min |
| SBN-2-4 | 1:2 | 1000 °C, 10 min and 10 °C/min |

$$0.5BaCO_3 + 0.5SrCO_3 + Nb_2O_5 = Sr_{0.5}Ba_{0.5}Nb_2O_6 + CO_2 \quad (1)$$

### 2.2. Characterization of SBN particles

Phase analyses were carried out in Rigaku X-ray diffractometer (RINT2550). The morphology and size distribution of particles were observed by SEM (JEOL, JSM-5600N) and laser scattering particle size distribution analyzer (HORIBA, LA-920S). In the laser particle size distribution analysis, the particles were dispersed in deionized water by ultrasonication for 4 min before the measurement. The electric diffraction of the particle were performed under a TEM (JEOL, JEM2010) equipped with EDS (ThermoNORAN, VANTAGE).

## 3. Results and discussion

### 3.1. Solid-state reaction synthesis

Fig. 1 shows SEM image of the SBN50 powder synthesized at 1300 °C by solid-state reaction. As indicated by arrow, the primary particle has a nearly spherical shape, and around 1 μm size. But they are strongly agglomerated, and some of them have become polycrystalline particles (as denoted grain boundary with circle). There are two peaks in the particle size distribution pattern (Fig. 2), a small one at around 1 μm, and a big one at around 6 μm. It should be noticed that some particles reach 30 μm even after a strong ultrasonic dispersion. These results indicate that most particles in SBN synthesized by solid-state reaction are polycrystalline or hard to be dispersed. They are difficult to be employed in the self-assemble processes.

### 3.2. Molten salt synthesis

#### 3.2.1. Phase development

Figs. 3 and 4 show the phase development of SBN-1 and SBN-2 compositions synthesized by MSS at designated tem-

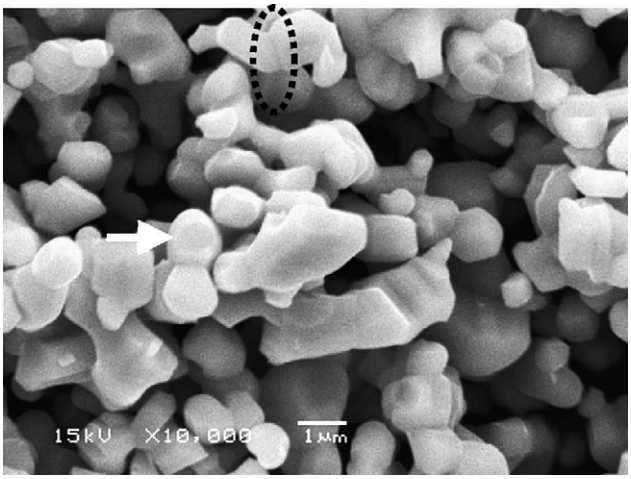


Fig. 1. Morphologies of SBN50 particles synthesized by solid-state reaction at 1300 °C.

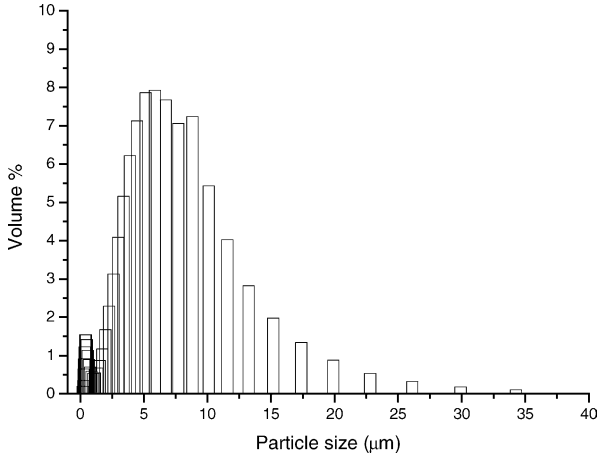


Fig. 2. Particle size distribution of SBN50 synthesized by solid-state reaction at 1300 °C.

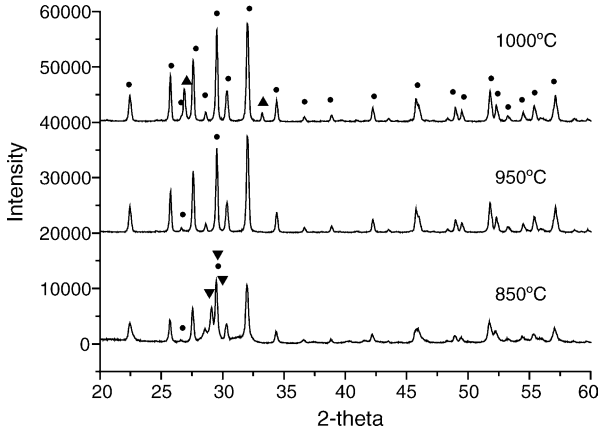


Fig. 3. Phase development of SBN-1composition synthesized by molten-salt method: (●) SBN50; (▼) $SrNb_2O_6/BaNb_2O_6$ and (▲) $Sr_2Nb_2O_7$.

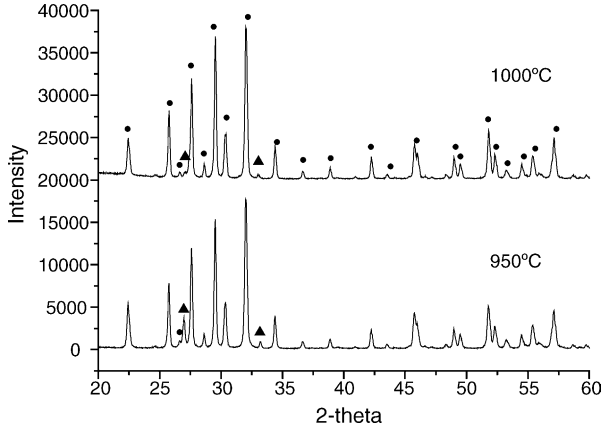


Fig. 4. Phase development of SBN-2 composition synthesized by molten-salt synthesis: (●) SBN50 and (▲) $Sr_2Nb_2O_7$.

peratures for 4 h, respectively. In SBN-1 composition, the peaks of $SrNb_2O_6$ and $BaNb_2O_6$ are still strong at 850 °C, but at 950 °C, only SBN50 phase is detected. So, the temperature to complete SBN formation is much lower in MSS than that in solid-state reaction, which normally lies between 1100 and 1200 °C.[20] This can be attributed mainly to the enhanced diffusivity of the constituent oxides in the liquid state of salt.[13] When temperature increases to 1000 °C, a minor amount of $Sr_2Nb_2O_7$ phase appears. This agrees with the results of Duran et al.[2] It should be noted that the $Sr_2Nb_2O_7$ phase also was detected in SBN-2, even at relatively low temperature 950 °C. Based on these results, we assume that high temperature and more amount of NaCl–KCl salt might accelerate the formation of $Sr_2Nb_2O_7$ phase. At these two situations, the cations of salt, $Na^+$ (1.39 Å) and $K^+$(1.64 Å),[21] may more easily substitute for $Sr^{2+}$ (1.54 Å) in SBN tungsten bronze structure. This point will be described in the later by TEM and EDS analysis.

### 3.2.2. *Morphological characterization of particles*

Figs. 5 and 6 show the effect of salt amount and temperature on the morphology and size distribution of the synthesized particles. From SEM results, the particle morphology and size do not change at different synthesis temperatures (950 and 1000 °C), but are influenced significantly by the salt amount. In both SBN-1 samples, particles show obvious anisotropic shape and have sizes at around 0.2–0.3 μm in diameter and 1 μm in length. In both SBN-2 samples, particles are still anisotropic in shape, but coarser in diameter and shorter in length, as comparison to SBN-1 samples. The laser particle size distribution analysis results further prove this fact. As indicated in Fig. 6, the median particle size ($d_{50}$) is around 0.47 μm in SBN-1 samples, and 0.55 μm in SBN-2 samples. In addition, the particle size distributions of all samples are very uniform, especially in SBN-1 samples. In comparison with the SBN particles synthesized by solid-state reaction, SBN particles synthesized from MSS are very fine, single crystalline and easily dispersed.

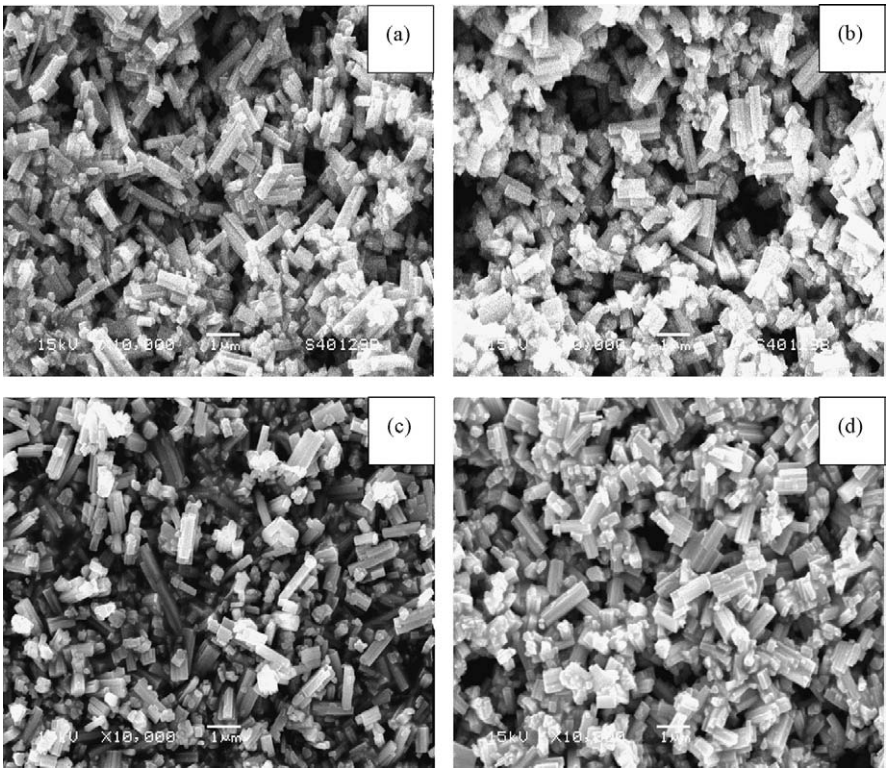


Fig. 5. Morphology of SBN particles synthesized at different temperatures and molten salt amounts: (a) SBN-1-1; (b) SBN-2-1; (c) SBN-1-2 and (d) SBN-2-2.

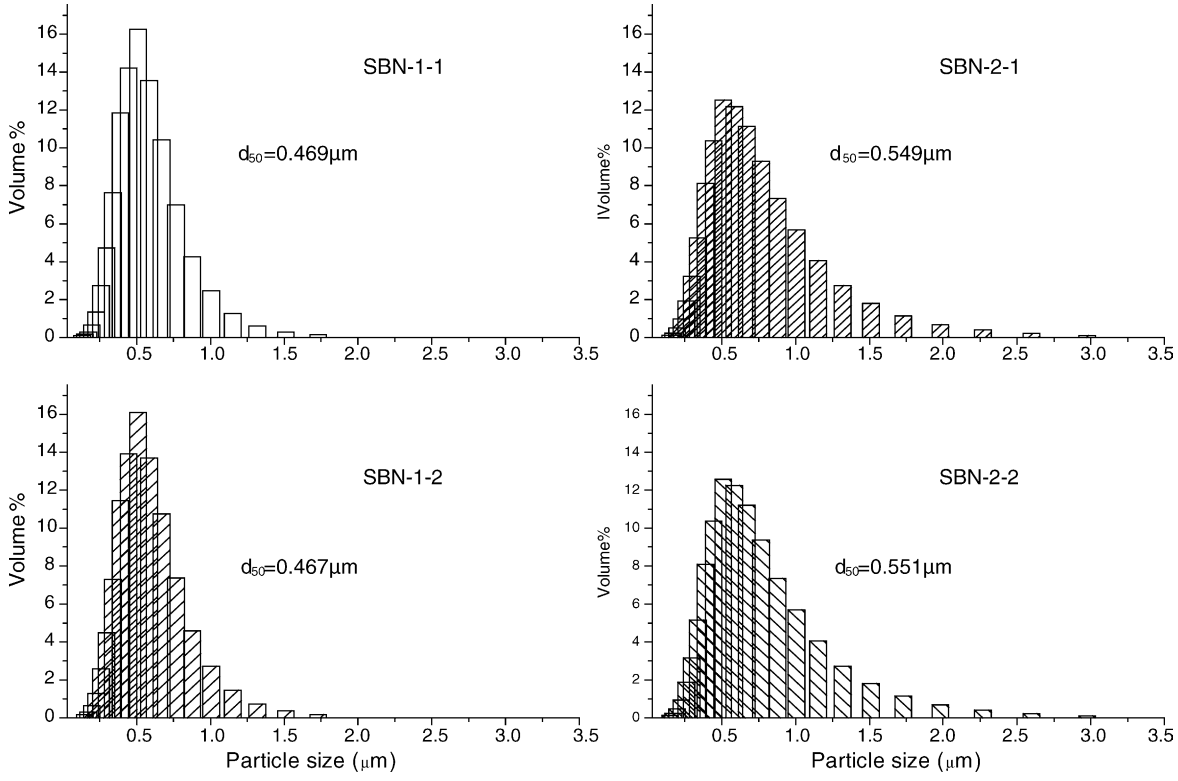


Fig. 6. Particle size distribution of SBN particles synthesized at different temperatures and molten salt amounts.

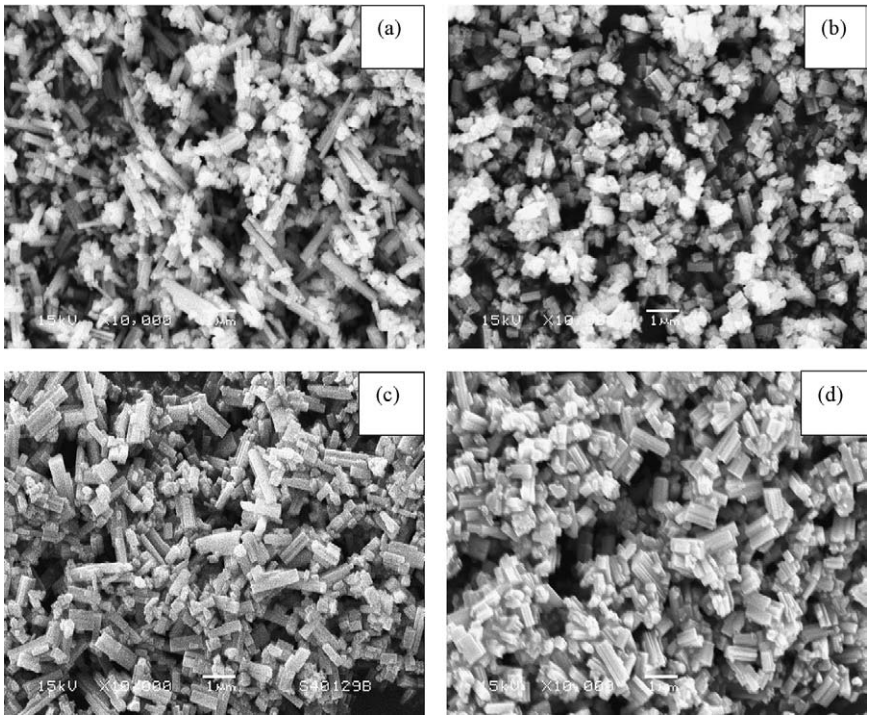


Fig. 7. Morphology of SBN particles synthesized with different processing parameters: (a) SBN-1-4; (b) SBN-2-4; (c) SBN-1-3 and (d) SBN-2-3.

Fig. 7 shows the effect of processing parameters on the morphology and size distribution of particles. At 1000 °C SBN-1-4 and SBN-2-4 samples were held for 10 min, and SBN-1-3 and SBN-2-3 samples were held for 4 h, before they were cooled down at 10 °C/min. In SBN-1-4 and SBN-2-4 samples, particles are finer and some of them may be still nuclei (not faceted morphology). With increasing holding time, the particles become coarser, longer and faceted. But the high cooling rate does not show much influence on the morphology when comparing the SBN-1-3 and SBN-2-3 with SBN-1-2 and SBN-2-2.

The formation of SBN particles in MSS is through a solution-precipitation process. Above the melting point of NaCl–KCl (650 °C), the oxides may start to dissolve and form a liquid containing cations and anions.[13] With increasing concentration of ions, the SBN may precipitate, and then particle growth occurs. In the present work, most SBN particles are faceted, which mean the grain growth is mainly controlled by the mass diffusion.[22–24] It has been accepted in single crystal growth that the morphology of crystal is determined by two factors: (1) the crystalline habit and (2) the driving force for grain growth.[22,23] SBN is tetragonal and has advantage in particle growth along *c*-axis. When the driving force for growth is low, the particle may grow according to its crystalline habit and show obvious anisotropic morphology, while if the driving force is too high, the particle has a trend to reduce the anisotropic growth and show an equiaxed shape. In MSS, the mass diffusion is related to the solubility, mobility and distance of ions in the molten salt. When the amount of salt is increased, the dissolution of starting powders may be accelerated, which improves the driving force for particle growth. Thus the particles show less anisotropic morphology with low aspect ratio. If the synthesis temperature is increased, the solubility and mobility of ions in molten salt should increase. But from the experimental results, this increase is not obvious between 950 and 1000 °C, so the morphologies of SBN particle change very little. In comparison to the rode-like particle of SBN-1-4 and SBN-1-3, the aspect ratio of SBN particles decreases slightly due to the diameter increasing with prolong soaking time. It seems that the aspect ratio of around 5 is the limited value for the particles in the SBN-1 composition synthesized at 1000 °C.

### *3.2.3. TEM characterization*

Single crystalline SBN particles (SBN-1-1) synthesized at 950 °C were investigated by TEM, as shown in Fig. 8. The electronic diffraction pattern further indicates that the SBN particles synthesized by MSS are single crystalline and has an advantage in growth along *c*-axis. The EDS spectrum, as shown in Fig. 9, indicates that $Na^+$ and $K^+$ ions enter into the SBN lattice. This is because of the close ionic radius of $Na^+$ (1.39 Å), $K^+$ (1.64 Å), $Sr^{2+}$ (1.54 Å) and $Ba^{2+}$ (1.74 Å). During the formation SBN50, $Na^+$ and $K^+$ ions also have the chance to take up the $A_1$ or $A_2$ position of SBN lattice. The strong Cu signal in EDS spectrum is attribute to cupper mesh as TEM sample holder. The influence of the incorporated $Na^+$ and $K^+$ on the physic properties of SBN will be studied lately.

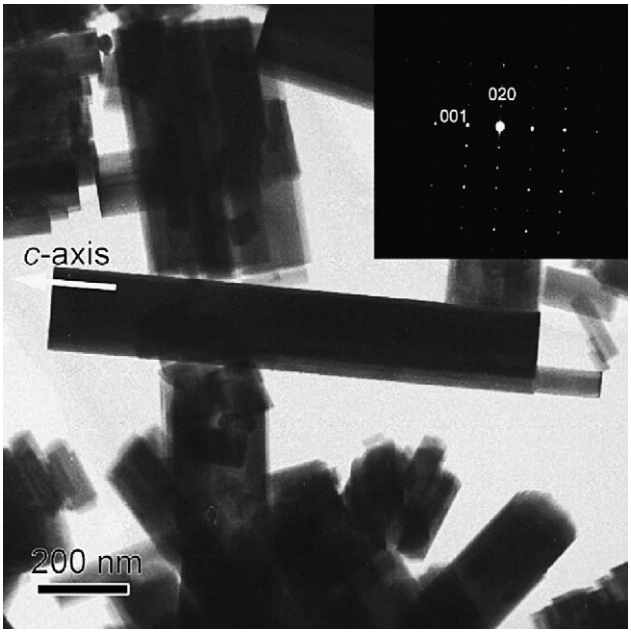


Fig. 8. TEM and electric diffraction of SBN single crystalline particle.

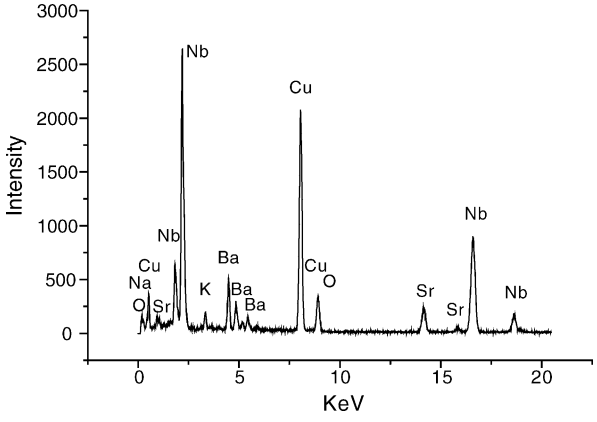


Fig. 9. EDS spectrum of SBN single SBN50 crystalline particle.

## 4. Conclusions

Single crystalline and agglomerate-free SBN50 particles were successfully prepared possibly by molten-salt synthesis, while solid-state reaction method resulted in severe agglomeration of particles. In MSS, pure SBN50 phase may be obtained at 950 °C and 1:1 weight ratio of oxides and salt. When the temperature and salt amount increase, $Sr_2Nb_2O_7$ phase starts to appear. The synthesized particles are faceted, sub-micrometer and have anisotropic morphology along *c*-axis. With increasing amount of salt, the aspect ratio of SBN particles are reduced, while the synthesis temperature does not show much influence on the particle morphology between 950 and 1000 °C. Incorporation of $Na^+$ and $K^+$ ions are found in SBN50 lattice. MSS-synthesized SBN50 particles are suitable for the preparation of grain-oriented ceramics by self-assemble processes.

## Acknowledgements

This work was supported by Japan Society for the Promotion of Science (JSPS) program. Weiwu Chen would like to thank Dr. Yu Jia and Dr. Kimiyasu Sato of AIST, for the assistance on experimental work.

## References

1. Sabolsky, E. M., James, A. R., Kwon, S., Trolier-Mckinstry, S. and Messing, G. L., Piezoelectric properties of ⟨0 0 1⟩ textured $Pb(Mg_{1/3}Nb_{2/3})O_3$–$PbTiO_3$ ceramics. *Appl. Phys. Lett.*, 2001, **78**, 2551–2553.
2. Duran, C., Trolier-Mckinstry, S. and Messing, G. L., Fabrication and electrical properties of textured $Sr0.53Ba0.47Nb_2O_6$ ceramics by templated grain growth. *J. Am. Ceram. Soc.*, 2000, **83**, 2203–2213.
3. Horn, J. A., Zhang, S. C., Selvaraj, U., Messing, G. L. and Trolier-McKinstry, S., Templated grain growth of textured bismuth titanate. *J. Am. Ceram. Soc.*, 1999, **82**, 921–926.
4. Sakka, Y., Suzuki, T., Tanabe, N., Asai, S. and Kitazawa, K., Alignment of titania whisker by colloidal filtration in a high magnetic field. *Jpn. J. Appl. Phys.*, 2002, **41L**, 1416–1418.
5. Uchikoshi, T., Suzuki, T., Okuyama, H. and Sakka, Y., Electrophoretic deposition of α-alumina particles in a strong magnetic field. *J. Mater. Res.*, 2003, **18**, 254–256.
6. Glass, A. M., Investigation of the electrical properties of $Sr_xBa_{1-x}Nb_2O_6$ with special reference to pyroelectric detection. *J. Appl. Phys.*, 1969, **40**, 4699–4713.
7. Ewbank, M. D., Neugaonkar, R. R., Cory, W. K. and Feinberg, J., Photorefractive properties of strontium–barium niobate. *J. Appl. Phys.*, 1987, **62**, 374–380.
8. Neugaonkar, R. R., Cory, W. K., Oliver, J. R., Sharp, E. J., Wood, G. L. and Salamo, G. J., Growth and optical properties of ferroelectric tungsten bronze crystals. *Ferroelectrics*, 1993, **142**, 167.
9. Nagata, K., Yamanoto, Y., Igarashi, H. and Okazaki, K., Properties of the hot-pressed strontium niobate ceramics. *Ferroelectrics*, 1992, **38**, 853.
10. Li, Y., Zhao, J. P. and Wang, B., Low temperature preparation of nanocrystalline powders $Sr_{0.5}Ba_{0.5}Nb_2O_6$ using an aqueous organic gel route. *Mater. Res. Bull.*, 2004, **39**, 365–374.
11. Hirano, S., Yogi, T., Kikuta, K. and Ogiso, K., Preparation of strontium barium niobate by sol–gel method. *J. Am. Ceram. Soc.*, 1992, **75**, 1697.
12. Lu, S. G., Mak, C. L. and Wong, K. H., Low temperature preparation and size effect of strontium barium niobate ultrafine powder. *J. Am. Ceram. Soc.*, 2001, **84**, 79–84.
13. Yoon, K. H., Cho, Y. S. and Kang, D. H., Review: Molten salt synthesis of lead-based relaxors. *J. Mater. Sci.*, 1998, **33**, 2977–2984.
14. Brahmaroutu, B., Messing, G. L. and Trolier-McKinstry, S., Molten salt synthesis of anisotropic $Sr_2Nb_2O_7$ particles. *J. Am. Ceram. Soc.*, 1999, **82**, 1565–1568.
15. Arendt, R. H., The molten salt synthesis of single magnetic domain $BaFe_{12}O_{19}$ and $SrFe_{12}O_{19}$ crystal. *J. Solid State Chem.*, 1973, **8**, 339–347.
16. Katayama, K., Azuma, Y. and Takahashi, Y., Molten salt synthesis of single-phase $BaNd_2Ti_4O_{12}$ powder. *J. Mater. Sci.*, 1999, **34**, 301–305.
17. Aboujalil, A., Deloume, J. P., Chassagneux, F., Schaff, J. P. and Durand, B., Molten salt synthesis of the lead titanate $PbTiO_3$, investigation of the reactivity of various titanium and lead salts with molten alkali-metal nitrites. *J. Mater. Chem.*, 1998, **8**, 1601–1606.
18. Li, C. C., Chiu, C. C. and Desu, S. B., Formation of lead niobates in molten salt systems. *J. Am. Ceram. Soc.*, 1991, **74**, 42–47.
19. Wan, D. M., Wang, J., Ng, S. C. and Gan, L. M., Formation and characterization of lead magnesium niobate synthesis from the

molten salt of potassium chlorate. *J. Alloys Compd.*, 1998, **274**, 110–117.
20. Qua, Y. Q., Li, A. D., Shao, Q. Y., Tang, Y. F., Wu, D., Mak, C. L. *et al.*, Structure and electrical properties of strontium barium niobate ceramics. *Mater. Res. Bull.*, 2002, **37**, 503–513.
21. Shannon, R. D., Revised effective ionic radii and systematic studied of interatomic distances in halides and chalcogenides. *Acta Cryst.*, 1976, **A32**, 751–767.
22. Hartman, P. and Bennema, P., The attachment energy as a habit controlling factor. I. Theoretical considerations. *J. Cryst. Growth*, 1980, **49**, 145–156.
23. Chernov, A. A., Rashkovich, L. N. and Mkrtchan, A. A., Solution growth kinetics and mechanism: prismatic face of ADP. *J. Cryst. Growth*, 1986, **74**, 101–112.
24. Kang, S. J. L. and Han, S. M., Grain growth in $Si_3N_4$-based materials. *MRS Bull.*, 1995, **20**, 33–36.